Title: Expansion of a fly TBI model to four levels of injury severity reveals synergistic effects of repetitive injury for moderate injury conditions

Authors: Lauren J Putnam*, Ashley M Willes*, Brooke E Kalata*, Nathaniel D Disher*, Douglas J Brusich

* = authors contributed equally to this work

Author Affiliations: Human Biology, College of Science, Engineering, and Technology, University of Wisconsin – Green Bay, Green Bay, WI, USA

Corresponding Author: Dr. Douglas J Brusich, brusichd@uwgb.edu

Running Title: Expansion of a fly TBI model and synergistic effects

ABSTRACT

Several million traumatic brain injury (TBI) events are reported in the United States annually. However, mild TBI events often go unreported, and mild and repetitive mild TBI conditions are challenging to model. Fruit flies (*Drosophila melanogaster*) have gained traction for the study of TBI. The best-characterized fly TBI model is the high-impact trauma (HIT) method. We replicated the HIT method and confirmed several previous findings at the standard level of injury severity. We then expanded upon the HIT model by characterizing mortality across three reduced levels of injury severity. Importantly, we found reduced mortality with reduced injury severity and synergistic effects on mortality in response to repetitive TBI by our moderate injury conditions. Last, we compared moderate, repetitive TBI to a single severe TBI via assessment of the pattern of mortality and geotaxis performance in the 24 h following TBI. We found the number and severity of injuries could result in different patterns of death, while all TBI conditions led to impaired geotaxis compared to uninjured flies at 0.5 h and 6 h post-TBI. Thus, we have extended a well-characterized model of TBI in flies, and shown the utility of this model for making unique insights into TBI across various severities, injury numbers, and time-points post-injury.

Keywords: traumatic brain injury, TBI, repetitive injury, mortality, geotaxis, Drosophila, injury severity

INTRODUCTION

In the United States, traumatic brain injury (TBI) annually accounts for greater than 2.5 million emergency room (ER) visits, hospitalizations, and deaths combined (Taylor et al. 2017). Additionally, half of all mild TBI events are estimated to go unreported (Cassidy et al. 2004). Mild TBI events, including concussion and sub-concussive impacts, are commonly suffered during sports participation and military deployment (Marar et al. 2012; Helmick et al. 2015; Kerr et al. 2017; Baldwin et al. 2018). Individuals in contact sports such as football may experience greater than one thousand mild head impacts per year, while approximately 10% of U.S. Army soldiers reported multiple mild TBI events from a previous deployment (Crisco et al. 2010; Wilk et al. 2012).

Severe TBI events are associated with long-term outcomes including greater risk for dementia, and are associated with many hallmarks of neurodegenerative disease (DeKosky and Asken 2017; Nordström and Nordström 2018). Individual mild TBI events are not well-linked to long-term outcomes, and most TBI-associated conditions resolve within months, particularly in children (Holm et al. 2005). By contrast, repetitive mild TBI is associated with more prominent impairment or disease, such as a greater risk of neurodegenerative disease in American football players (Lehman et al. 2012; Bailes et al. 2013; Levin and Robertson 2013). Moreover, rodent models of repetitive mild TBI result in neurocognitive deficits, and histological and morphological changes associated with neurodegenerative disease (Mouzon et al. 2012; Ojo et al. 2016; Gold et al. 2018). Importantly, additional TBI events suffered within days of the first injury result in more negative outcomes due to the combination of primary and secondary injury mechanisms (Laurer et al. 2001; Longhi et al. 2005; Friess et al. 2009; Meehan et al. 2012; Huang et al. 2013; Bolton and Saatman 2014; Weil et al. 2014; Bolton Hall et al. 2016).

Two models for studying TBI have been developed for the fruit fly (*Drosophila melanogaster*): the high-impact trauma (HIT) method, which uses a spring-based device deflected to 90°, and the Bead Ruptor homogenizer method, which uses a programmable homogenizer that can be set to various speeds and durations (Katzenberger et al. 2013; Barekat et al. 2016). Importantly, use of each method results in classic post-TBI symptoms including impaired locomotion, shortened lifespan, neurodegeneration, intestinal barrier disruption, and activation of immune and autophagy processes (Katzenberger et al. 2013; Barekat et al. 2016; Anderson et al. 2018). While the Bead Ruptor method offers potential advantages in the ease of scaling primary injuries and inter-experiment standardization, the HIT method is simple, cost-effective, and

better characterized to date (Katzenberger et al. 2013, 2015, 2016; Barekat et al. 2016; Anderson et al. 2018).

We sought to standardize the HIT method across several levels of injury severity, thereby extending this well-characterized method to the study of mild to severe TBI events in an easily replicable manner. To this end, we installed fixed, selectable stopping points that limited deflection of the HIT device to either 60º, 70º, 80º, or 90º. We found that reducing the angle of deflection greatly reduced mortality, and that repetitive injury at moderate levels of severity resulted in a pronounced synergistic effect on mortality. Moreover, we found that the pattern of death in the 24 h post-TBI could be affected by the nature of repetitive injury. Last, we found that locomotion was impaired when assessed at an early 0.5 h time-point and also during the secondary injury window at 6 h post-TBI, but was no different than controls when assessed 2 h or 24 h post-TBI.

MATERIALS AND METHODS

Fly Husbandry

Flies of genotype w^{1118} (BL 5905) and y^1w^1 (BL 1495) were obtained from the Bloomington Drosophila Stock Center (Bloomington, Indiana , USA). Flies were maintained in a 25°C humidified incubator on a 12H:12H light:dark cycle. Flies were maintained on a glucose-cornmeal-yeast media with the following quantities per 1.25L of water: 7.66g agar (Apex), 14.4g glucose (DOT Scientific Inc.), 50.3g cornmeal (Genesee), 15g yeast (Genesee), 5.66mL tegosept (Genesee), 4.67mL propionic acid (99%, Acros Organics), and 0.47mL phosphoric acid (85%, Matheson Coleman & Bell Inc.).

TBI Methodology

Flies were collected using light-CO_2 anesthesia. Flies were subjected to traumatic brain injury on or before 5 days after eclosion (dae) using an adapted model of the high-impact trauma (HIT) device (Katzenberger et al. 2013). Briefly, flies were transferred to an empty vial and the vial was affixed to the end of a compression spring. The vial was deflected to a selectable, fixed stopping point of 60°, 70°, 80° or 90°. The vial was released and allowed to collide with a foam pad covered by a 1/16” rubber pad. Vial deflections were repeated every 15 seconds for the total number of deflections indicated. Flies were immediately hand-transferred to a food vial following the final injury. Uninjured flies were handled identically minus spring deflection and injury. The number of dead flies were counted at designated time-points ranging from 30 minutes post-injury to 24 h post-injury. Flies counted at 24 h post-injury were used to determine the mortality index at 24 h (MI_{24}) (MI_{24} = # flies dead at 24 h post-injury/total # flies * 100). The MI_{24}/HIT values were determined using the MI_{24} divided by total number of injuries for the condition.

Negative Geotaxis

Flies aged 0-4 dae were collected under light-CO_2 anesthesia and transferred to food vials. Animals were subjected to TBI, following the same methods as above, and geotaxis testing, at a designated time post-TBI, a minimum of 1 day after CO_2 exposure. Individual vials of flies were tested at a single time-point each and a minimum of 5 vials were used for each time-point. Prior to geotaxis testing, flies were hand-transferred to empty vials and given 10 minutes undisturbed on the geotaxis platform to recover prior to experimentation. Vial plugs were kept to within the top 10mm of the vial.

A custom-built geotaxis apparatus which accommodated up to 6 vials simultaneously was used for all geotaxis testing. Briefly, the device consisted of wood and plywood construction affixed to two ring stands used as vertical runners. Geotaxis behavior was initiated by startle whereby the device was lifted to stops on the ring stands which allowed approximately 95mm of vertical movement, dropped, and the process repeated twice more for a total of 3 drops in quick succession. Foam pads were used to cushion both the device and the platform upon which the vials rested. Vials were held in place on the device by use of elastic cords placed around the top 10mm of the vial. A webcam (Logitech c270) was used to record each experiment.

VLC media player (version 3.0.6) with a self-written subtitle file displaying the video time to the tenths of seconds was used for analysis. Screenshots were taken at 5.0 s and 10.0 s after the 3rd drop. Screenshots were processed in ImageJ (1.47v/Java 1.6.0_20 (32-bit)). Three lines were drawn to measure the height of the vial in pixels and averaged. The Cell Counter plug-in was used to mark vial bottoms and flies for each sample. Pixel coordinates from Cell Counter were combined with the pixel measure of the vial and the known length of the vial (95mm) to convert each fly's pixel coordinate to a distance traveled from the vial bottom in millimeters. Distance measurements were capped at 50mm. GraphPad Prism 7 software (GraphPad Software, Inc.) was used to generate a histogram of distance measures and bin values into 12.5mm quartiles. Dead flies were not included in geotaxis measurements.

Statistics

Pairwise comparisons of categorical (dead:alive) count data were performed using a 2x2 Fisher's Exact Test between selected conditions (GraphPad Prism 7). Bonferroni correction was used to correct for multiple testing and corrected alpha levels are reported in figure legends. Comparisons of median MI_{24}/HIT values and geotaxis data were conducted via Kruskal-Wallis testing (GraphPad Prism 7) with multiple comparisons of mean ranks and Dunn's correction at a level of $\alpha = 0.05$. Only vials containing at least 30 flies were used in median MI_{24}/HIT comparisons. Full count data were used for comparisons of trends across MI_{24}/HIT data; overall MI_{24} values were divided by their respective HIT number, plotted across 1-4HITs, and fitted using the linear fit mode within the nonlinear regression analysis toolkit (GraphPad Prism 7). Lines were fitted using the least squares fit mode, compared to a hypothetical slope of zero via the extra sum-of-squares F test at a level of $\alpha = 0.05$, and the 95% confidence interval (CI) determined asymmetrically. Dead fly counts from determination of death across time-points were compared by Fisher's Exact Tests of 4x2 matrices in R (version 3.5.1) with post-hoc, pairwise comparisons (dead within window:dead outside of window) via 2x2 Fisher's Exact

Tests (GraphPad Prism 7). Bonferroni correction was used to correct for multiple post-hoc testing and the corrected alpha level is reported in the text or figure legend.

RESULTS

Replication of 90º HIT data

The primary measure of TBI outcomes in flies is the percentage of flies that die within 24 hours post-injury (MI_{24}). We first set out to determine how our TBI system and resulting MI_{24} values compared to existing models. We conducted experiments using a 90º angle of deflection and two strains of fruit fly, w^{1118} and y^1w^1, for which y^1w^1 was previously reported to suffer higher MI_{24} (Katzenberger et al. 2013). Vials of flies were subjected to 0-4 high-impact traumatic injuries (HITs) (see Table 1 for all categorical count data). Uninjured flies suffered little or no mortality at 24 h, while administration of 1-4HITs resulted in pronounced MI_{24} with increased death upon increased HIT number (Fig. 1A, shared letters indicate statistical significance between conditions). Comparisons across genotypes showed MI_{24} values of w^{1118} and y^1w^1 flies were no different for uninjured controls, but y^1w^1 flies suffered greater mortality than w^{1118} flies for each of the 1-4HIT datasets (Fig. 1A, (*) indicates differences between genotypes).

It was previously reported that MI_{24} values divided by HIT number (MI_{24}/HIT) were no different from one another when compared across a range of HITs (Katzenberger et al. 2013). We carried out the same comparisons for our datasets and found differences for median MI_{24}/HIT values for w^{1118} (Fig. 1B, 1HIT vs 3HIT) and y^1w^1 (Fig. 1C, 1HIT vs 3HITs, and 1HIT vs 4HITs). The differences in MI_{24}/HIT prompted us to look more closely at the pattern of change in mortality across HIT numbers. If mortality is directly proportional to the number of flies which experience a critical injury for each HIT then we would expect the MI_{24}/HIT values compared across HIT numbers to have a zero slope. We used overall count data to determine MI_{24}/HIT values and then fitted these points across 1-4 HITs with a linear best-fit model. At 90º we found that neither w^{1118} nor y^1w^1 had slopes that significantly deviated from zero (Table 2).

Expansion to three levels of reduced injury severity

In order to expand the range of primary injury severities by the HIT method, we added additional, fixed, selectable stopping points to reduce the angle of deflection to 80°, 70°, or 60°. We again assessed MI_{24} outcomes by independently administering 1-4HITs at each of the three new angles of deflection. We found lower MI_{24} values in each of the new deflection angles when compared to 90° within both w^{1118} and y^1w^1 datasets at each of 1-4HITs (Fig. 2A-D respectively). We also found significantly reduced MI_{24} with each reduction in deflection angle from 80° to 70° and then 70° to 60° at each of 2-4 HITs within both w^{1118} and y^1w^1 datasets (Figs. 2B-D), while genotype-specific differences across deflection angle were seen at 1HIT (Fig. 2A). Moreover, in

both genotypes we found the MI_{24} from 1HIT at 60°, our most mild injury severity, was not significantly different than the MI_{24} in uninjured animals using a significance level of $\alpha = 0.005$ after Bonferroni correction (Fig. 2A, p-values: $w^{1118} = 0.39$, $y^1w^1 = 0.03$). Last, we found y^1w^1 flies suffered greater mortality than w^{1118} flies at all deflection angles when 3 or 4 HITs were administered (Figs. 2C and 2D). However, differences between genotypes were only statistically different at the 80º and 90º deflection angles when injuries were limited to 1 or 2 HITs (Figs. 2A and 2B). Nonetheless, y^1w^1 flies appeared comparatively more sensitive to TBI at less severe primary injuries as the fold-difference in y^1w^1:w^{1118} MI_{24} values progressively decreased from 3.84-fold at 60º to 1.53-fold at 90º for 4HITs (Fig. 2D), a pattern similarly observed for other HIT numbers.

Synergistic effects are apparent for repetitive injury at moderate TBI severity

We continued our analysis of the additional deflection angles to comparisons of MI_{24}/HIT values. We found differences in MI_{24}/HIT values when comparing 1HIT and 4HITs in both w^{1118} and y^1w^1 at each of the sub-90º deflection angles (Fig. 3). Additionally, differences between both 1HIT and 3HITs, and 2HITs and 4HITs were also seen for w^{1118} at 80° (Fig. 3A) and y^1w^1 at 70° (Fig. 3D). We again investigated trends in MI_{24}/HIT data from 1-4HITs via analysis of slopes from best-fit lines. If mortality was strictly additive for each HIT then the trend across MI_{24}/HIT data should generate a zero-slope line. However, at both 80º and 70º, but not 60º, both w^{1118} and y^1w^1 had positive, significantly non-zero slopes, indicating a synergistic effect on mortality (Table 2). The positive slopes and synergistic effects were most evident at moderate severity injuries of 80º for w^{1118} (1.82 +/- 0.05 (SE)) and 70º for y^1w^1 (2.08 +/- 0.42 (SE)) (Table 2).

Time-Course of Mortality

Animals subjected to TBI experience both primary injury from the TBI event itself and secondary injuries related to cellular and molecular events instigated by the primary injury. The secondary injury period in flies reportedly peaks between 1 h and 8 h post-injury and persists for at least 24 h (Katzenberger et al. 2016). We hypothesized that the relative contributions of primary and secondary injuries on mortality would differ when comparing a single severe injury (90º x 1HIT) to repetitive injury at less severe angles. By our data, injury via 90º x 1HIT results in similar MI_{24} values as 80º x 2HITs and 70º x 3HITs, particularly for y^1w^1 flies (Table 1), thereby giving us conditions by which to test our hypothesis while keeping overall MI_{24} values comparable. We injured new cohorts of flies by these 3 conditions and recorded mortality post-TBI at times which corresponded to an early, pre-secondary injury window (0.5 h), early peak of the secondary

injury period (2 h), delayed peak of the secondary injury period (8 h), and late secondary injury period (24 h).

We found the only conditions which generated different patterns in the time-course of death were 80º x 2HITs vs 90º x 1HIT, and this was true for both the w^{1118} and y^1w^1 genotypes (Fig. 4). Notably, while the overall trends between the two conditions differed for w^{1118} there were no pairwise differences by post-hoc testing (Fig. 4). By contrast, y^1w^1 flies showed significantly greater late death from 8 h – 24 h when injured by 80º x 2HITs vs. 90º x 1HIT (Fig. 4). Injury via 70º x 3HITs resulted in no differences in the time-course of death compared to either the 80º x 2HITs or 90º x 1HIT conditions for either genotype (Fig. 4).

Last, we compared the pattern of death between the w^{1118} and y^1w^1 genotypes. We found the pattern of death from both the 70º x 3HITs and 80º x 2HITs differed between genotypes (Figs. 4A and 4B; 70º: $p = 0.010$, 80º: $p = 0.002$, $\alpha = 0.017$ by 4x2 Fisher's Exact Test with Bonferroni correction). By pairwise comparisons of the 70º x 3HIT datasets, we found that w^{1118} flies suffered a greater proportion of death by 0.5 h post-TBI than y^1w^1 flies ($p = 0.001$, $\alpha = 0.0125$ by 2x2 Fisher's Exact Test with Bonferroni correction). Alternately, y^1w^1 flies suffered greater death during the 2+ h to 8 h period than w^{1118} flies by comparison of 80º x 2HITs datasets ($p = 0.004$, $\alpha = 0.0125$ by 2x2 Fisher's Exact Test with Bonferroni correction).

Time-Course of Motor Dysfunction

Flies are well-known to exhibit motor dysfunction following TBI (Katzenberger et al. 2013; Barekat et al. 2016; Anderson et al. 2018). However, the time-course of motor dysfunction across the primary and secondary injury periods, and for TBI of varying severities is not well-characterized. Therefore, we extended our characterization of outcomes across several time-points and the 70º x 3HITs, 80º x 2HITs, and 90º x 1HIT conditions via a negative geotaxis assay. We restricted our analysis to w^{1118} flies which have been best-characterized via this assay to date. We also opted to use a 6 h post-TBI time-point in place of the 8 h time-point used for the time-course of mortality to better capture outcomes during the middle of the peak of the secondary injury window.

We determined geotaxis performance by measuring the distance traveled by each fly 5 seconds and 10 seconds after startle, which were similar time-points to previous literature (Gargano et al. 2005; Linderman et al. 2012; Podratz et al. 2013; Anderson et al. 2018). All conditions showed improved scores at 10 s compared to 5 s (Fig. 5, $p < 0.05$, $\alpha = 0.5$, Kruskal-Wallis with Dunn's correction). In comparing conditions, we found that w^{1118} flies subjected to any of the three TBI

conditions showed impaired geotaxis compared to uninjured flies at both the 0.5 h and 6 h post-TBI time-points, but not 2 h or 24 h post-TBI time-points, for each of the 5 s and 10 s measures (Fig. 5, see (*)). However, we observed no differences in geotaxis performance between any of the TBI conditions at any of the time-points tested. Comparisons within TBI conditions and across time-points showed a general trend for improved geotaxis scores at 2 h compared to 0.5 h post-TBI (Fig. 5A: see 'a' and 'b', Fig. 5B: see 'a', 'b', and 'd'), followed by a second impairment in geotaxis for both the 70º x 3HITs and 80º x 2HITs datasets at 6 h post-TBI when assessed at 5 s post-startle (Fig. 5A, see 'c' and 'd').

DISCUSSION

Fruit flies offer an accessible model to study TBI. Two models of conducting TBI studies in fruit flies are the high-impact trauma (HIT) method and the Bead Ruptor method (Katzenberger et al. 2013; Barekat et al. 2016). One advantage to the Bead Ruptor method is the ease of scaling the primary injuries (Barekat et al. 2016). We addressed this gap in methodology and expanded upon the original HIT method by adding selectable stopping points to reproducibly perform injury at four levels of injury severity. We then applied our expanded methodology to characterization of the time-course of death and locomotor dysfunction in the 24 h following TBI.

Several of our main findings are in agreement with the established TBI models. First, we found that increasing the injury number results in dose-dependent increases in mortality (Figs. 1 and 3) (Katzenberger et al. 2013; Barekat et al. 2016; Anderson et al. 2018). Second, we found that y^1w^1 flies suffer greater mortality than w^{1118} flies subjected to the same injuries, and we extended this finding to our mild and moderate TBI conditions (Figs. 1 and 2) (Katzenberger et al. 2013). Notably, our MI_{24} values at the standard protocol of 90º x 4HITs (Table 1, w^{1118}: 53.3%; y^1w^1: 81.6%) were not identical to previous literature (w^{1118}: ~30%; y^1w^1: ~50%) (Katzenberger et al. 2013; Anderson et al. 2018), likely due to lab specific differences such as variation in the force generated by the spring and/or the features of the collision surface. However, it is notable that we reproduced the data showing increased sensitivity of y^1w^1 flies (Katzenberger et al. 2013), thereby demonstrating the reliability of this TBI model and the penetrance of unknown genetic influences (Katzenberger et al. 2015). Third, we found that reducing the angle of deflection resulted in less severe primary injuries as indicated by decreased mortality, and extended this finding across the four levels of deflection tested (Fig. 2) (Anderson et al. 2018). Fourth, we found that TBI led to diminished locomotor ability that returned to normal levels by 24 h post-TBI (Fig. 5) (Katzenberger et al. 2013).

Several of our findings are also novel for this TBI system. First, we found a synergistic effect of additional HITs on mortality by our moderate TBI conditions and short inter-injury intervals (15 seconds) (Table 2). It was previously reported that dividing the MI_{24} by the number of HITs resulted in no differences when comparing across HIT number (Katzenberger et al. 2013). This result was used as evidence that the main factor influencing MI_{24} across multiple HITs was the likelihood of suffering a critical injury for each HIT, and that secondary injury mechanisms were negligible for injuries spaced closely together as the secondary injury window does not peak until 1-8 h after injury (Katzenberger et al. 2013, 2016). By contrast, we found differences when comparing median MI_{24}/HIT values even at these close (15 second) inter-injury intervals (Figs. 1B, 1C, 3A-F). Additionally, we looked more closely at the pattern of MI_{24}/HIT values across HIT number. If only primary injuries, and not secondary injuries or increased susceptibility to mortality due to preceding strikes, were responsible for observed MI_{24} values then the MI_{24}/HIT values across HIT number should generate a zero slope line. At 90º neither w^{1118} nor y^1w^1 had significantly non-zero best-fit line slopes, consistent with properties of the primary injury being most responsible for MI_{24} at these severe injury levels and short inter-injury interval (Table 2). By contrast, for our moderate severity injuries at 80º and 70º, both w^{1118} and y^1w^1 MI_{24}/HIT data generated positive, significantly non-zero slopes, indicating a synergistic effect of HIT number on mortality. This result suggests that secondary injury mechanisms, or increased susceptibility to injury due to preceding injuries, contributed to MI_{24} (Table 2). A non-zero trend in MI_{24}/HIT data was not observed for injuries at 60º, though it is possible that such a trend would be evident if injury number was further increased as the MI_{24} value increased noticeably between 3 and 4 HITs for both w^{1118} and y^1w^1 (Table 2).

A second novel finding was the pattern of death in the 24 h following TBI. First, we found a difference in the pattern of death when comparing 80º x 2HITs to 90º x 1HIT within both w^{1118} and y^1w^1 genotypes (Fig. 4). Interestingly, we observed an increased proportion of death in the late period from 8+ h to 24 h post-TBI in the 80º x 2HIT dataset for y^1w^1 flies (Fig. 4A), and a similar, nonsignificant trend for w^{1118} flies (Fig. 4B). This finding is consistent with our initial hypothesis that repetitive, moderate injury would lead to a greater proportion of death in the secondary injury period than a single, severe TBI event. However, by contrast to this finding, we found no differences when comparing the pattern of death via 70º x 3HITs to 90º x 1HIT (Fig. 4).

Why might 2HITs at the 80º deflection angle, but not 3HITs at 70º, cause a different pattern of death than 1HIT at 90º? One possibility is the presence of separate secondary injury mechanisms, one operating on a short time-scale (seconds) and the other the previously

defined mechanism operating on a longer time-scale (hours) (Katzenberger et al. 2016). By this model, the administration of 2HITs at 80º causes significant secondary injuries on the longer time-scale and greater death after 8+ h compared to 1HIT at 90º (Fig. 4B). By contrast, 70º x 3HITs and the synergistic secondary effects on the short time-scale exceeds a critical threshold and causes early death before the classic secondary injury period. Such a two-stage secondary injury model may also be applicable to differences between genotypes. By our data, the most common period of death for w^{1118} flies regardless of TBI condition was within 0.5 h of injury, while for y^1w^1 flies it was during the typical secondary injury period from 2+ h to 8 h for 70º x 3HITs and 90º x 1HIT datasets and 8+ h to 24 h for the 80º x 2HITs dataset. This data suggests that w^{1118} flies are more susceptible to fast secondary injury mechanisms (seconds), while y^1w^1 flies are more susceptible to the later secondary injury mechanisms (hours). Consistent with this, administration of 70º x 3HITs to each genotype revealed a significant increase in the proportion of death by the 0.5 h time-period for w^{1118} as compared to the proportion for y^1w^1 flies (Fig. 4), consistent with a threshold sensitive to fast secondary injury mechanisms in the genotype more sensitive to these changes. By contrast, the 80º x 2HIT condition which may not exceed the early threshold, caused an increase in death during the later, classic secondary injury period from 2+ h to 8 h in y^1w^1 flies more susceptible to these mechanisms.

Our final novel finding was the more detailed pattern of locomotor dysfunction in the 24 h following TBI and for isolated vs repetitive TBI conditions. We found that flies showed early locomotor dysfunction at 0.5 h compared to uninjured flies for all three TBI conditions tested, but found no differences between TBI conditions at this early time-point (Fig. 5). We then saw a trend for improved geotaxis scores that were no different than controls by the early stages of the classic secondary injury period at 2 h post-TBI and during the delayed secondary injury period 24 h post-TBI, consistent with previous results for 1-2HITs at 90º (Katzenberger et al. 2013) (Fig. 5). More interesting and novel were the impaired geotaxis scores for injured flies at 6 h post-TBI, a time corresponding to the middle of the secondary injury period. However, diminished geotaxis scores at 6 h post-TBI were only different than 2 h scores for the repetitive TBI conditions of 70º x 3HITs and 80º x 2HITs (Fig. 5A). Thus, all TBI conditions led to early geotaxis impairment and a second impairment during the secondary injury window at 6 h post-TBI, while the secondary period difference at 6 h post-TBI was most noted in the repetitive TBI conditions.

What are the mechanisms by which closely spaced, mild or moderate injuries synergistically affect TBI outcomes? Secondary mechanisms might include autophagy-related pathways and

stress granule formation (Anderson et al. 2018). In fly larvae, stress granules were not apparent after single TBI events at 60º, minimally increased after 4HITs, and substantially increased after 8HITs in an apparently synergistic fashion (Anderson et al. 2018). Alternatively, glutamate release and elevated extracellular potassium are observed immediately or within minutes of TBI (Faden et al. 1989; Katayama et al. 1990). Moreover, extracellular potassium scaled with injury severity until plateauing for severe injuries, and changes in extracellular potassium were blocked by addition of tetrodotoxin for moderate but not severe injuries (Katayama et al. 1990). Thus, dysregulation of neuronal excitability and extracellular potassium operate on short time-scales and are responsive to injury severity, which are compatible with our observed synergistic effects for injuries at short inter-injury intervals and for moderate, but not severe TBI. Downstream consequences of misregulated neurotransmission and extracellular potassium are varied, but may include changes in oxidative stress and inflammation (Guerriero et al. 2015; Fehily and Fitzgerald 2017; Khatri et al. 2018).

Our evidence for synergistic effects of mild to moderate TBI and short inter-injury intervals is of consequence to mammals. In mammals the secondary injury window is typically reported as within days post-injury (Laurer et al. 2001; Longhi et al. 2005; Friess et al. 2009; Meehan et al. 2012; Huang et al. 2013; Bolton and Saatman 2014; Weil et al. 2014; Bolton Hall et al. 2016). However, the number of sub-concussive events suffered by individuals across a short time-scale, a single American football game, correlated with short-term blood-brain-barrier damage (Marchi et al. 2013). Thus, mild TBI events suffered in number across a short time-scale may be an important factor to consider for brain health, especially considering the large number (> 1,000) of sub-concussive injuries suffered during football participation across a season of play (Crisco et al. 2010).

The exact secondary mechanisms underlying the fast synergistic effects we observed are thus far unknown. Moreover, we do not know if synergistic effects at mild to moderate TBI conditions in our model drive other TBI-related consequences observed in flies such as changes in lifespan and inflammation (Katzenberger et al. 2013, 2015, 2016; Barekat et al. 2016; Anderson et al. 2018). However, our fly model offers an unparalleled platform for rapidly, and systematically, testing candidate factors or pathways for their involvement in TBI outcomes across injury severities, number, and inter-injury interval. Recognition and elucidation of cellular and molecular differences in response to mild vs moderate, single vs multiple TBI events, and across varying time-scales will be important in determining optimal disease-intervention strategies. Our extended model will be central to these efforts going forward.

Acknowledgements: The authors thank members of the Human Biology Department at the University of Wisconsin – Green Bay for careful reading of the manuscript and suggested revisions. We also thank Dr. C. Andrew Frank, Dr. Tina Tootle, Dr. Atulya Iyengar, and Dr. Javier Gomez for reading the manuscript and offering revisions, and for their support in answering many questions about lab set-up and publication. We also thank Mark Damie and Joe Schoenebeck of the University of Wisconsin – Green Bay for assistance in lab set-up.

Declarations of Interests: The authors have no conflicts of interest.

Funding: This work was supported by University of Wisconsin – Green Bay Start-Up Funds, University of Wisconsin – Green Bay Summer Scholar Grant, and Medical College of Wisconsin Professional Development Funds.

LITERATURE CITED

Anderson EN, **Gochenaur L**, **Singh A**, **Grant R**, **Patel K**, **Watkins S**, **Wu JY**, **Pandey UB**. Traumatic injury induces stress granule formation and enhances motor dysfunctions in ALS/FTD models. *Human Molecular Genetics* 27: 1366–1381, 2018.

Bailes JE, **Petraglia AL**, **Omalu BI**, **Nauman E**, **Talavage T**. Role of subconcussion in repetitive mild traumatic brain injury. *Journal of Neurosurgery* 119: 1235–1245, 2013.

Baldwin GT, **Breiding MJ**, **Dawn Comstock R**. Epidemiology of sports concussion in the United States. In: *Handbook of clinical neurology*. 2018, p. 63–74.

Barekat A, **Gonzalez A**, **Mauntz RE**, **Kotzebue RW**, **Molina B**, **El-Mecharrafie N**, **Conner CJ**, **Garza S**, **Melkani GC**, **Joiner WJ**, **Lipinski MM**, **Finley KD**, **Ratliff EP**. Using Drosophila as an integrated model to study mild repetitive traumatic brain injury. *Scientific Reports* 6: 25252, 2016.

Bolton AN, **Saatman KE**. Regional Neurodegeneration and Gliosis Are Amplified by Mild Traumatic Brain Injury Repeated at 24-Hour Intervals. *Journal of neuropathology and experimental neurology* 73: 933, 2014.

Bolton Hall AN, **Joseph B**, **Brelsfoard JM**, **Saatman KE**. Repeated Closed Head Injury in Mice Results in Sustained Motor and Memory Deficits and Chronic Cellular Changes. *PLOS ONE* 11: e0159442, 2016.

Cassidy JD, **Carroll LJ**, **Peloso PM**, **Borg J**, **von Holst H**, **Holm L**, **Kraus J**, **Coronado VG**, **WHO Collaborating Centre Task Force on Mild Traumatic Brain Injury**. Incidence, risk factors and prevention of mild traumatic brain injury: results of the WHO Collaborating Centre Task Force on Mild Traumatic Brain Injury. *Journal of rehabilitation medicine* : 28–60, 2004.

Crisco JJ, **Fiore R**, **Beckwith JG**, **Chu JJ**, **Brolinson PG**, **Duma S**, **McAllister TW**, **Duhaime A-C**, **Greenwald RM**. Frequency and Location of Head Impact Exposures in Individual Collegiate Football Players. *Journal of Athletic Training* 45: 549–559, 2010.

DeKosky ST, **Asken BM**. Injury cascades in TBI-related neurodegeneration. *Brain Injury* 31: 1177–1182, 2017.

Faden AI, **Demediuk P**, **Panter SS**, **Vink R**. The role of excitatory amino acids and NMDA receptors in traumatic brain injury. *Science (New York, NY)* 244: 798–800, 1989.

Fehily B, **Fitzgerald M**. Repeated Mild Traumatic Brain Injury. *Cell Transplantation* 26: 1131–1155, 2017.

Friess SH, **Ichord RN**, **Ralston J**, **Ryall K**, **Helfaer MA**, **Smith C**, **Margulies SS**. Repeated traumatic brain injury affects composite cognitive function in piglets. *Journal of neurotrauma* 26: 1111–21, 2009.

Gargano J, **Martin I**, **Bhandari P**, **Grotewiel M**. Rapid iterative negative geotaxis (RING): a new method for assessing age-related locomotor decline in. *Experimental Gerontology* 40: 386–395, 2005.

Gold EM, **Vasilevko V**, **Hasselmann J**, **Tiefenthaler C**, **Hoa D**, **Ranawaka K**, **Cribbs DH**, **Cummings BJ**. Repeated Mild Closed Head Injuries Induce Long-Term White Matter Pathology and Neuronal Loss That Are Correlated With Behavioral Deficits. *ASN Neuro* 10: 175909141878192, 2018.

Guerriero RM, **Giza CC**, **Rotenberg A**. Glutamate and GABA imbalance following traumatic brain injury. *Current neurology and neuroscience reports* 15: 27, 2015.

Helmick KM, **Spells CA**, **Malik SZ**, **Davies CA**, **Marion DW**, **Hinds SR**. Traumatic brain injury in the US military: epidemiology and key clinical and research programs. *Brain Imaging and Behavior* 9: 358–366, 2015.

Holm L, **David Cassidy J**, **Carroll L**, **Borg J**, **Neurotrauma Task Force on Mild Traumatic Brain Injury of the WHO Collaborating Centre**. Summary of the WHO collaborating centre for neurotrauma task force on mild traumatic brain injury. *Journal of Rehabilitation Medicine* 37: 137–141, 2005.

Huang L, **Coats JS**, **Mohd-Yusof A**, **Yin Y**, **Assaad S**, **Muellner MJ**, **Kamper JE**, **Hartman RE**, **Dulcich M**, **Donovan VM**, **Oyoyo U**, **Obenaus A**. Tissue vulnerability is increased following repetitive mild traumatic brain injury in the rat. *Brain Research* 1499: 109–120, 2013.

Katayama Y, **Becker DP**, **Tamura T**, **Hovda DA**. Massive increases in extracellular potassium and the indiscriminate release of glutamate following concussive brain injury. *Journal of Neurosurgery* 73: 889–900, 1990.

Katzenberger RJ, **Chtarbanova S**, **Rimkus SA**, **Fischer JA**, **Kaur G**, **Seppala JM**, **Swanson LC**, **Zajac JE**, **Ganetzky B**, **Wassarman DA**. Death following traumatic brain injury in Drosophila is associated with intestinal barrier dysfunction. *eLife* 4, 2015.

Katzenberger RJ, **Ganetzky B**, **Wassarman DA**. Age and Diet Affect Genetically Separable Secondary Injuries that Cause Acute Mortality Following Traumatic Brain Injury in Drosophila. *G3 (Bethesda, Md)* 6: 4151–4166, 2016.

Katzenberger RJ, **Loewen CA**, **Wassarman DR**, **Petersen AJ**, **Ganetzky B**, **Wassarman DA**. A Drosophila model of closed head traumatic brain injury. *Proceedings of the National Academy of Sciences of the United States of America* 110: E4152-9, 2013.

Kerr ZY, **Roos KG**, **Djoko A**, **Dalton SL**, **Broglio SP**, **Marshall SW**, **Dompier TP**. Epidemiologic Measures for Quantifying the Incidence of Concussion in National Collegiate Athletic Association Sports. *Journal of Athletic Training* 52: 167, 2017.

Khatri N, **Thakur M**, **Pareek V**, **Kumar S**, **Sharma S**, **Datusalia AK**. Oxidative Stress: Major Threat in Traumatic Brain Injury. *CNS & neurological disorders drug targets* 17: 689–695, 2018.

Laurer HL, **Bareyre FM**, **Lee VMYC**, **Trojanowski JQ**, **Longhi L**, **Hoover R**, **Saatman KE**, **Raghupathi R**, **Hoshino S**, **Grady MS**, **McIntosh TK**. Mild head injury increasing the brain's vulnerability to a second concussive impact. *Journal of Neurosurgery* 95: 859–870, 2001.

Lehman EJ, **Hein MJ**, **Baron SL**, **Gersic CM**. Neurodegenerative causes of death among retired National Football League players. *Neurology* 79: 1970–1974, 2012.

Levin HS, **Robertson CS**. Mild traumatic brain injury in translation. *Journal of neurotrauma* 30: 610–7, 2013.

Linderman JA, **Chambers MC**, **Gupta AS**, **Schneider DS**. Infection-Related Declines in Chill Coma Recovery and Negative Geotaxis in Drosophila melanogaster. *PLoS ONE* 7: 41907, 2012.

Longhi L, **Saatman KE**, **Fujimoto S**, **Raghupathi R**, **Meaney DF**, **Davis J**, **McMillan B S A**, **Conte V**, **Laurer HL**, **Stein S**, **Stocchetti N**, **McIntosh TK**. Temporal window of vulnerability to repetitive experimental concussive brain injury. *Neurosurgery* 56: 364–74, 2005.

Marar M, **McIlvain NM**, **Fields SK**, **Comstock RD**. Epidemiology of Concussions Among United States High School Athletes in 20 Sports. *The American Journal of Sports Medicine* 40: 747–755, 2012.

Marchi N, **Bazarian JJ**, **Puvenna V**, **Janigro M**, **Ghosh C**, **Zhong J**, **Zhu T**, **Blackman E**, **Stewart D**, **Ellis J**, **Butler R**, **Janigro D**. Consequences of Repeated Blood-Brain Barrier Disruption in Football Players. *PLoS ONE* 8: e56805, 2013.

Meehan WP, **Zhang J**, **Mannix R**, **Whalen MJ**. Increasing Recovery Time Between Injuries Improves Cognitive Outcome After Repetitive Mild Concussive Brain Injuries in Mice. *Neurosurgery* 71: 885–892, 2012.

Mouzon B, **Chaytow H**, **Crynen G**, **Bachmeier C**, **Stewart J**, **Mullan M**, **Stewart W**, **Crawford F**. Repetitive Mild Traumatic Brain Injury in a Mouse Model Produces Learning and Memory Deficits Accompanied by Histological Changes. *Journal of Neurotrauma* 29: 2761–2773, 2012.

Nordström A, **Nordström P**. Traumatic brain injury and the risk of dementia diagnosis: A nationwide cohort study. *PLoS medicine* 15: e1002496, 2018.

Ojo JO, **Mouzon B**, **Algamal M**, **Leary P**, **Lynch C**, **Abdullah L**, **Evans J**, **Mullan M**, **Bachmeier C**, **Stewart W**, **Crawford F**. Chronic Repetitive Mild Traumatic Brain Injury Results in Reduced Cerebral Blood Flow, Axonal Injury, Gliosis, and Increased T-Tau and Tau Oligomers. *Journal of Neuropathology and Experimental Neurology* 75: 636, 2016.

Podratz JL, **Staff NP**, **Boesche JB**, **Giorno NJ**, **Hainy ME**, **Herring SA**, **Klennert MT**, **Milaster C**, **Nowakowski SE**, **Krug RG**, **Peng Y**, **Windebank AJ**, **Windebank AJ**. An automated climbing apparatus to measure chemotherapy-induced neurotoxicity in Drosophila melanogaster. *Fly* 7: 187–92, 2013.

Taylor CA, **Bell JM**, **Breiding MJ**, **Xu L**. Traumatic Brain Injury–Related Emergency Department Visits, Hospitalizations, and Deaths — United States, 2007 and 2013. *MMWR Surveillance Summaries* 66: 1–16, 2017.

Weil ZM, **Gaier KR**, **Karelina K**. Injury timing alters metabolic, inflammatory and functional outcomes following repeated mild traumatic brain injury. *Neurobiology of Disease* 70: 108–116, 2014.

Wilk JE, **Herrell RK**, **Wynn GH**, **Riviere LA**, **Hoge CW**. Mild Traumatic Brain Injury (Concussion), Posttraumatic Stress Disorder, and Depression in U.S. Soldiers Involved in Combat Deployments. *Psychosomatic Medicine* 74: 249–257, 2012.

493 **Table 1:** Full reporting of categorical count data for all TBI conditions.

Genotype	Angle of Deflection	HITs	Alive @ 24 h	Dead @ 24 h	MI_{24}
w^{1118}	0 – uninjured	0 – uninjured	1325	0	0.0
y^1w^1	0 – uninjured	0 – uninjured	1256	3	0.2
w^{1118}	60°	1	837	1	0.1
		2	1453	9	0.6
		3	1104	9	0.8
		4	864	33	3.7
y^1w^1	60°	1	806	8	1.0
		2	959	16	1.6
		3	807	29	3.5
		4	748	124	14.2
w^{1118}	70°	1	1108	15	1.3
		2	1391	55	3.8
		3	984	71	6.7
		4	797	138	14.8
y^1w^1	70°	1	887	18	2.0
		2	962	47	4.7
		3	773	164	17.5
		4	524	236	31.1
w^{1118}	80°	1	689	19	2.7
		2	1313	128	8.9
		3	887	201	18.5
		4	570	277	32.7
y^1w^1	80°	1	733	64	8.0
		2	718	156	17.8
		3	561	265	32.1
		4	334	343	50.7
w^{1118}	90°	1	568	66	10.4
		2	985	386	28.2
		3	602	512	46.0
		4	342	390	53.3
y^1w^1	90°	1	735	137	15.7
		2	607	312	33.9
		3	283	459	61.9
		4	105	467	81.6

494 **Table 2:** Full reporting of line-fit slopes for MI_{24}/HIT data and resulting p-values.

Genotype	Angle of Deflection	Slope +/- SE	95% CI of slope	Significantly non-zero slope?	p-value
w^{1118}	60	0.24 +/- 0.1	-0.18 to 0.66	no	0.136
y^1w^1	60	0.81 +/- 0.42	-1.00 to 2.61	no	0.195
w^{1118}	70	0.74 +/- 0.17	0.02 to 1.46	**yes**	**0.048**
y^1w^1	70	2.08 +/- 0.42	0.28 to 3.89	**yes**	**0.038**
w^{1118}	80	1.82 +/- 0.05	1.61 to 2.03	**yes**	**0.001**
y^1w^1	80	1.57 +/- 0.18	0.81 to 2.33	**yes**	**0.013**
w^{1118}	90	1.00 +/- 0.90	-2.87 to 4.86	no	0.382
y^1w^1	90	1.77 +/- 0.50	-0.37 to 3.92	no	0.071

495

Figure 1

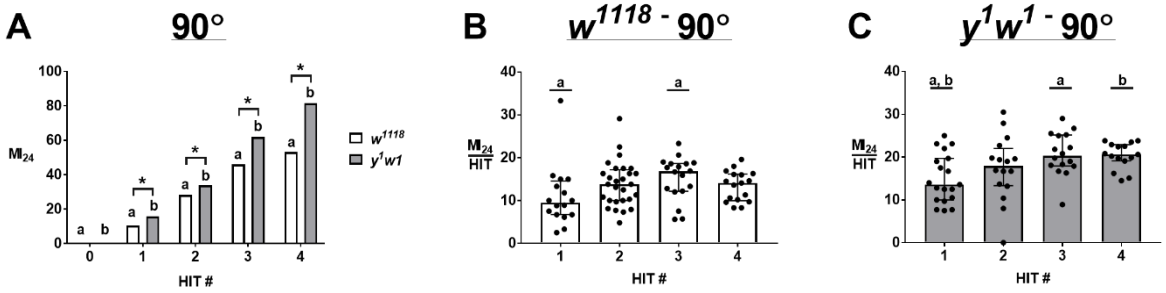

Figure 2

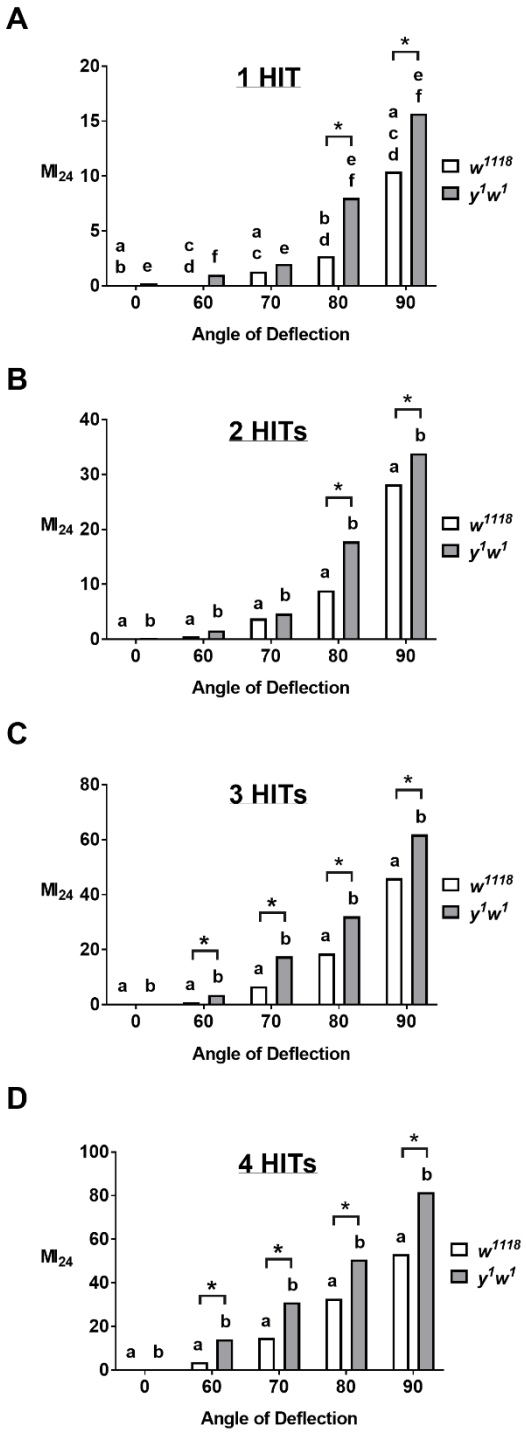

Figure 3

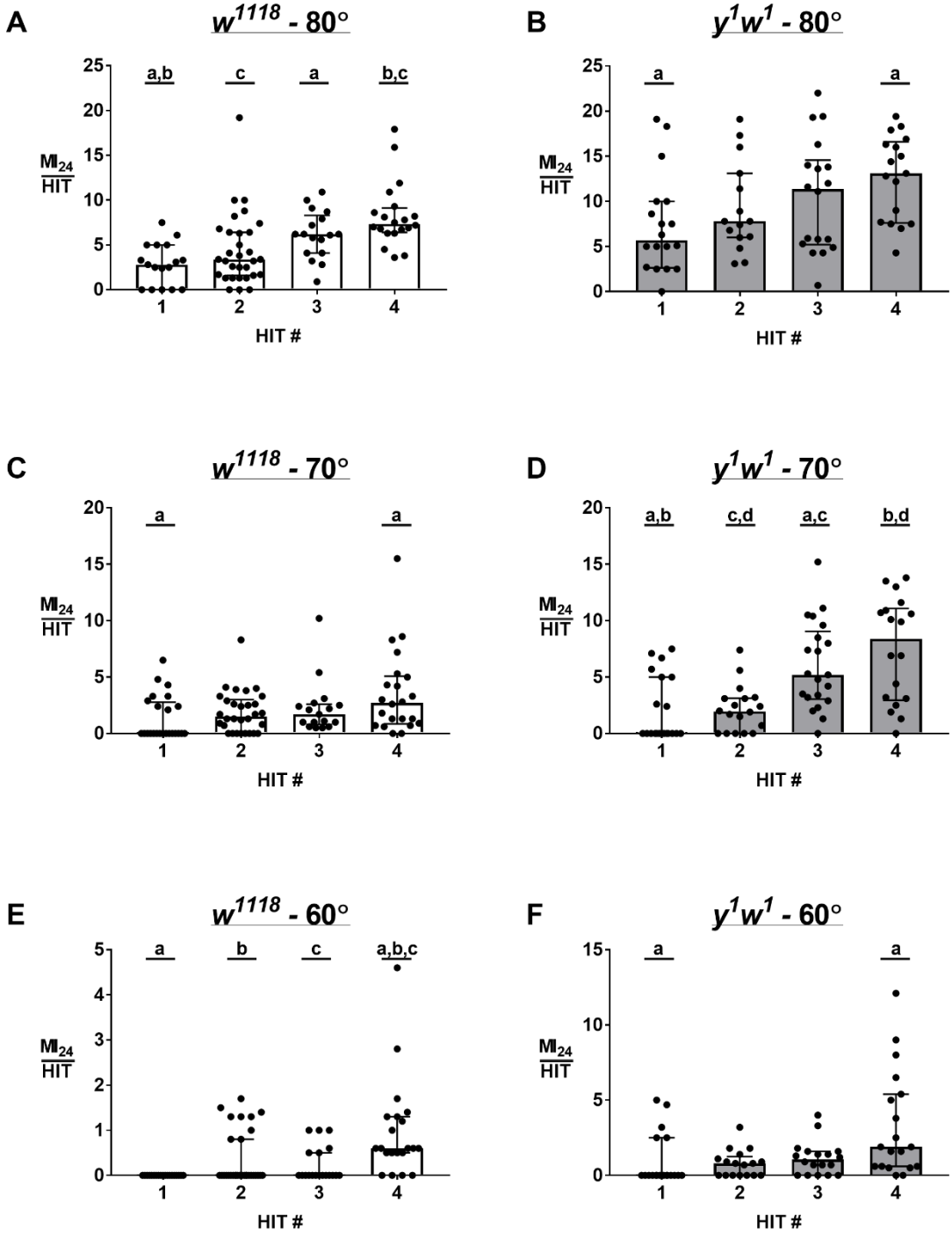

Figure 4

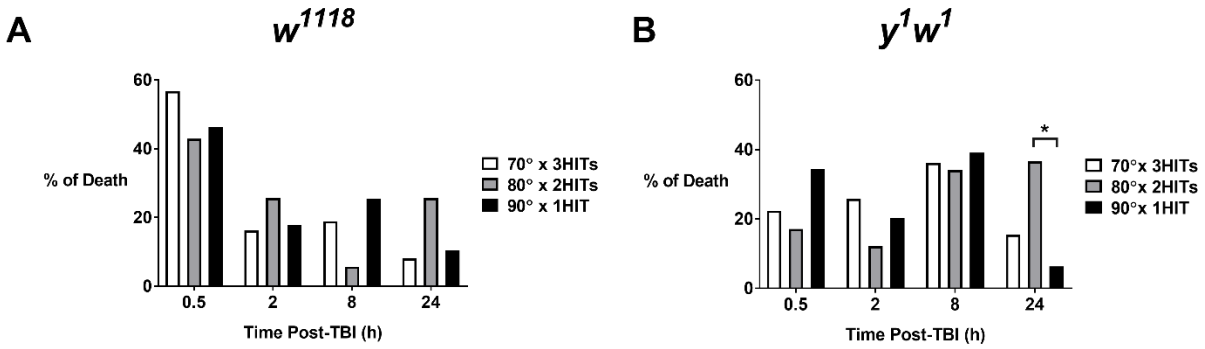

504 **Figure 5**

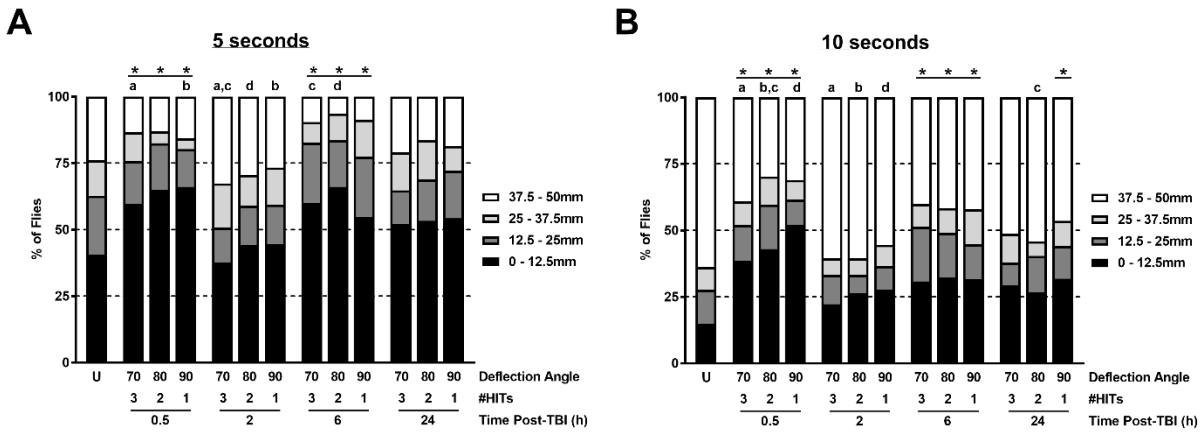

505

Figure 1: Increasing HIT number at 90º deflection increases MI_{24} and reveals differences in MI_{24} per hit. (A) MI_{24} values increase with HIT number in both w^{1118} and y^1w^1, with y^1w^1 suffering greater MI_{24} across all HIT numbers. Zero HITs represents uninjured controls. Conditions that share a letter are statistically different ($p \leq 0.0023$, $\alpha = 0.005$), while (*) indicates differences between genotypes ($p \leq 0.0029$, $\alpha = 0.01$) by Fisher's Exact Test with Bonferroni correction. $n \geq 572$ flies for each condition. (B, C) MI_{24} values were divided by HIT number for w^{1118} (B) and y^1w^1 (C). Data plotted are medians with interquartile ranges, with individual data points for each vial of at least 30 flies. Conditions that share a letter are statistically different ($p < 0.05$, $\alpha = 0.05$ by Kruskal-Wallis with Dunn's correction, $n \geq 15$ vials for each condition).

Figure 2: Mortality is reduced at smaller angles of deflection. Flies were administered 1-4HITs (A-D as indicated) at designated angles of deflection from 60º to 90º. Zero degrees represents uninjured controls. Conditions that share a letter are statistically different ($p \leq 0.0042$, $\alpha = 0.005$), while (*) indicates differences between genotypes ($p \leq 0.0035$, $\alpha = 0.01$) by Fisher's Exact Test with Bonferroni correction. $n \geq 572$ flies for each condition.

Figure 3: Differences in MI_{24} per hit are readily apparent for sub-90º injury conditions. MI_{24} values were divided by HIT number for w^{1118} and y^1w^1 as indicated at angles of deflection of 80º (A, B), 70º (C, D) and 60º (E,F). Data plotted are medians with interquartile ranges, with individual data points for each vial of at least 30 flies. Conditions that share a letter are statistically different ($p < 0.05$, $\alpha = 0.05$ by Kruskal-Wallis with Dunn's correction). $n \geq 15$ vials for each condition.

Figure 4: The time-course of mortality differs for 80º x 2HITs vs 90º x 1HIT. w^{1118} (A) and y^1w^1 (B) flies were injured by one of three designated conditions and the percentage of total death by 24 h post-injury is plotted for each of 4 time-points. Datasets of 80º x 2HITs vs 90º x 1HIT differed for each genotype ($p = 0.026$ for w^{1118}, $p = 0.001$ for y^1w^1, $\alpha = 0.05$ by 4x2 Fisher's Exact Test), while (*) indicates a difference via post-hoc pairwise comparison ($p < 0.001$, $\alpha = 0.0125$ by Fisher's Exact Test with Bonferroni correction). $n \geq 276$ flies per condition.

Figure 5: w^{1118} flies subjected to TBI exhibit time-dependent geotaxis impairment. Distances traveled by flies at 5 seconds (A) and 10 seconds (B) after startle were binned into 12.5mm quartiles for uninjured flies (U) and each TBI condition and assessed time post-TBI (h) indicated. Conditions that share a letter are statistically different, while (*) indicates a statistical difference between uninjured flies and the indicated condition ($p \leq 0.029$, $\alpha = 0.05$ by Kruskal-Wallis with Dunn's correction). $n \geq 101$ flies per condition.